Servo Performance of a BLDC Drive with Instantaneous Torque Control

Teck-Seng Low, Tong-Heng Lee, King-Jet Tseng, and Kai-Sang Lock

Abstract—**Brushless dc (BLDC) drives with permanent-magnet motors are suitable as servo motors if properly controlled. Their performance can be superior to conventional dc servos if NdFeB or rare-earth cobalt magnets are used for motor excitation, and novel control techniques implemented for its servo performance. The availability of inexpensive by high-performance digital signal processors allow the implementation of a novel instantaneous torque control algorithm for BLDC drive applications. This paper presents the servo performances of a BLDC drive with instantaneous torque control. To assess the quality of this controller, its performance is compared with those obtained using conventional current controllers. Details of the control strategies are also described.**

I. Introduction

BRUSHLESS dc (BLDC) drives using high torque permanent-magnet (PM) motors are suitable for direct drive applications in servo systems and robots. The advantages of direct drive systems lie in their ability to minimize the friction and backlash associated with geared drives [1]–[4]. However, the absence of gearing is not without its own problems. Direct drives have to operate at low speeds, where the effects of torque pulsations become particularly objectionable [5], [6]. However, with high-performance digital signal processors (DSP's) and fast switching power devices, it is now possible to implement an instantaneous torque controller as the inner loop controller with the outer loop responsible for the eventual speed or position response of the servo system [7]–[9]. This will give a close control of the torque characteristic and hence superior servo performance.

Conventional current controllers aimed to force the stator phase currents to be as close to the reference supplied (usually an ideal sinusoid) as possible for a constant torque command. These are usually synthesized from a hybrid combination of analog and digital devices. However, in many cases, the rotor flux distribution may not be exactly sinusoidal, resulting in torque pulsations [10]. The motor also operates under suboptimal conditions. The concept of instantaneous torque control for a BLDC drive is illustrated in Fig. 1. The combination of the three-phase inverter and the PM motor is regarded as a torque producing unit that accepts a 3-b digital command from the torque controller. The instantaneous torque feedback signal can be estimated from the knowledge of machine parameters and the measurements of instantaneous currents and rotor position. Thus, by designing appropriate control algorithms, it is possible to eliminate torque pulsations by using the direct digital control of the inverter. This would also lead to the optimal operation of the motor in the BLDC drive system and result in improved performance.

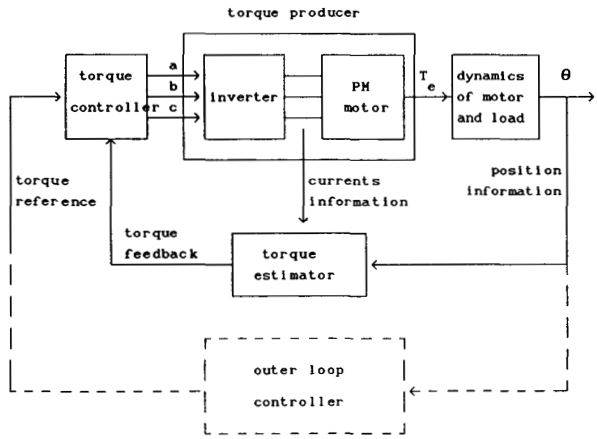

Fig. 1. Concept of instantaneous torque control.

This paper describes the performances of a BLDC drive for servo applications using the instantaneous torque control. The applications examined here are speed, position, and static torque control. Comparisons are made with respect to those obtained using the conventional current control. Details of their implementations are also given.

II. Control Strategies

A. Torque Control [7]

The torque control algorithm is based on the variable structure strategy (VSS) in which the switching signals for the inverter are determined directly by the digital controller. In the VSS system, a switching control law is used to drive the plant's state trajectory onto a chosen surface in the state space. This surface is known as the switching surface. In the BLDC drive, the *d-q* transformation is performed on the motor model so that the states are the direct-axis and quadrature-axis currents i_d and i_q.

The switching surfaces are selected to be

$$s_d = i_{dref} - i_d \tag{1}$$

Paper IPCSD 91-58, approved by the Industrial Drives Committee of the IEEE Industry Applications Society for presentation at the 1990 Industry Applications Society Annual Meeting, Seattle, WA, October 7–12. Manuscript released for publication April 16, 1991.

T.-S. Low, T.-H. Lee, and K.-S. Lock are with the Department of Electrical Engineering, National University of Singapore, Singapore.

K.-J. Tseng is with Cambridge University, Cambridge, England.

IEEE Log Number 9104090.

$$s_q = T_{ref} - T_e \tag{2}$$

where $i_{dref} = 0$ (for optimal BLDC operation), and T_{ref} is the torque reference as determined by the outer loop controller.

The VSS control functions are selected to be

$$V_d = V_d \operatorname{sgn}(s_d) \tag{3}$$

$$V_q = V_q \operatorname{sgn}(s_q). \tag{4}$$

These selections are based on the concept of vector control. The controller determines the control inputs v_d and v_q, which are in the rotating $d - q$ domain, by considering the positions of the state trajectories in the switching plane. There are four possible combinations of v_d and v_q. Their effects can be classified as in Table I. These control inputs are then mapped into the *abc* voltage vectors of the inverter. The results of the mapping are shown in Table II. Fig. 2 shows the block diagram of the torque controller.

1) Torque Estimation: The torque control scheme described in Section II-A requires an accurate instantaneous torque feedback signal. It is not feasible to measure the developed motor torque directly with torque transducers due to the difficulties involved in obtaining a reliable signal. In addition, typical torque transducers are usually bulky and have low bandwidths in their dynamic response. (Higher end torque transducers with the fast response needed for torque control are very costly.) In our implementation, we obtain the required instantaneous torque feedback signal by using least squares parameter estimation to obtain the motor torque parameters during a self-calibration phase and calculating, in real-time, the value from the appropriate torque equation.

For a PM motor with nonsinusoidal flux distribution, the torque feedback signal is described by the following equation:

$$T_e = \frac{3}{2}\frac{P}{2}\left[K_0 + K_6 \cos 6\theta + K_{12} \cos 12\theta + \cdots\right] i_q$$

where P is the number of poles, and $K_0, K_6, K_{12} \cdots$ are functions of the self-inductance harmonics in the direct L_{dfn} and quadrature axis L_{qfn}, and i_f is the equivalent field excitation current. In order to obtain the value of the instantaneous torque from the above expression, we need to be able to first obtain the values of the coefficients $K_0, K_6, K_{12} \cdots$ This is done by taking the expression for the quadrature-axis voltage, writing it in a linear-in-the-parameter model form, and then using the least squares parameter estimation technique to obtain estimates for the coefficients $K_0, K_6, K_{12} \cdots$ The procedure is as follows:

1) Before the BLDC drive with instantaneous torque control can be used for closed-loop applications, a self-calibration routine must be first invoked. This consists of first capturing a time frame of voltage, current, and velocity data from a test run. For this test run, a random input signal (for example, a pseudorandom binary sequence or PRBS signal) is set as the input and applied directly using the switching inverter.

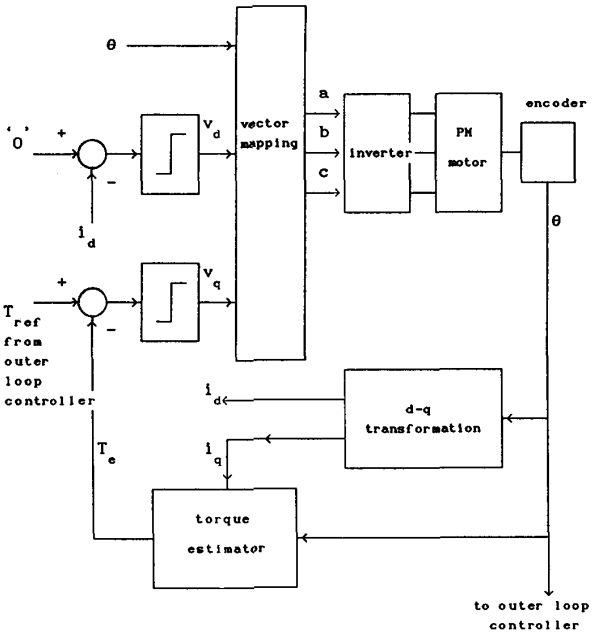

Fig. 2. Block diagram of torque controller.

TABLE I
CONTROL INPUTS AND ACTIONS

Control Inputs	Control Actions
$v_d = +V_d$, $v_q = +V_q$	increase i_d, increase i_q
$v_d = +V_d$, $v_q = -V_q$	increase i_d, decrease i_q
$v_d = -V_d$, $v_q = +V_q$	decrease i_d, increase i_q
$v_d = -V_d$, $v_q = -V_q$	decrease i_d, decrease i_d

TABLE II
MAPPING TO INVERTER VECTORS

	Inverter Vectors			
Rotor Angle	$v_d = +V_d$ $v_q = +V_q$	$v_d = -V_d$ $v_q = +V_q$	$v_d = -V_d$ $v_q = -V_q$	$v_d = +V_d$ $v_q = -V_q$
345-15°	1 1 0	0 1 0	0 0 1	1 0 1
15-45°	1 1 0	0 1 1	0 0 1	1 0 0
45-75°	0 1 0	0 1 1	1 0 1	1 0 0
75-105°	0 1 0	0 0 1	1 0 1	1 1 0
105-135°	0 1 1	0 0 1	1 0 0	1 1 0
135-165°	0 1 1	1 0 1	1 0 0	0 1 0
165-195°	0 0 1	1 0 1	1 1 0	0 1 0
195-225°	0 0 1	1 0 0	1 1 0	0 1 1
225-255°	1 0 1	1 0 0	0 1 0	0 1 1
255-285°	1 0 1	1 1 0	0 1 0	0 0 1
285-315°	1 0 0	1 1 0	0 1 1	0 0 1
315-345°	1 0 0	0 1 0	0 1 1	1 0 1

2) Using the time frame of signals capture above and the linear-in-the-parameter model

$$v_q = \begin{bmatrix} i_q & \dfrac{di_q}{dt} & \omega & \omega\cos 6\theta & \omega\cos 12\theta & \cdots \end{bmatrix} \begin{bmatrix} R \\ L_{qq0} \\ K_0 \\ K_6 \\ K_{12} \\ \vdots \end{bmatrix}$$

$$= \phi^T \alpha.$$

For the quadrature voltage, an off-line least squares calculation is used to yield estimates for $K_0, K_6, K_{12} \cdots$ Thus, if α is the vector of parameters as defined above, the least squares estimate is given by

$$\hat{\alpha} = \{\phi^T\phi\}^{-1}\phi^T Y$$

where ϕ is an appropriate matrix containing data from the time frame of signals, and Y is an appropriate vector containing quadrature voltage data. (For more complete details on obtaining the least squares estimate given a linear-in-the-parameters model, refer to any book on least squares parameter estimation.) For the PM motor that we used in our experiments, the torque harmonic coefficients are significant up to the sixth harmonic, i.e., $K_j = 0$ for $j > 6$. It is usually quite safe to start by including at least the first three harmonic coefficients K_0, K_6 and K_{12} and then checking their values to ascertain their level of significance. If necessary, an iterative procedure can then be used to determine the highest order harmonic coefficient that is still significant.

3) Having obtained the estimated torque harmonic coefficients, the BLDC drive is now ready for closed-loop operation with the instantaneous torque signal given by a real-time calculation using

$$T_e = \frac{3}{2}\frac{P}{2}\left[K_0 + K_6\cos 6\theta + K_{12}\cos 12\theta + \cdots\right] i_q.$$

It can be observed that the procedure above involves a self-calibration routine during the start-up phase. This effectively characterizes each motor before it is used in closed-loop applications and overcomes the effects of motor variations due to differences in components that are present even in parts (e.g., magnets) that come from the same lot.

It should also be mentioned that although the above procedure handles most of the problems arising from the effects of motor variation, there is one effect it does not address: the problem of the torque coefficients varying over time during operation due to temperature effects, for example. This is a more difficult problem that requires an on-line estimation procedure that continually keeps track of the torque coefficients instead of the one-shot off-line estimation procedure described above. One technique that can be used is the on-line recursive least squares estimator. Thus, if α is the vector of parameters to be estimated, the recursive least squares estimator has the structure

$$\hat{\alpha}(N+1) = \hat{\alpha}(N) + K(N)\left[v_q(N+1) - \phi(N+1)^T\hat{\alpha}(N)\right]$$

$$K(N) = P(N)\phi(N)\left[\rho + \phi(N)^T P(N)\phi(N)\right]^{-1}$$

$$P(N+1) = \frac{1}{\rho}\left[I - K(N)\phi(N+1)^T\right]P(N).$$

Here, ρ is an exponential weighting factor that discounts the effects of old data and ensures that the estimator tracks time-varying parameters. Although the necessary algorithmic details have all been resolved in our design, actual implementation using the on-line estimator has not yet been carried out in our experiments. We are at present using only the off-line one-shot self-calibrating version described above. This is because the algorithm is fairly computationally intensive. However, in current work, we are in the midst of instrumenting a microprocessor-based subsystem dedicated to implementing the recursive estimator and providing on-line estimates of the torque coefficients to be used in the torque calculation equation. Such a procedure will effectively handle the situation where the torque coefficients vary over time.

B. Speed Control

The torque controller for the inner loop can be coupled to a speed controller implemented for the outer loop. To assess the performances of such a system for speed control, a digital PI speed control algorithm is designed and incorporated as the outer loop controller. Fig. 3 shows the block diagram of the PI speed controller and the BLDC drive. The inner loop of the BLDC drive is modeled as a zero order hold. The z transform of the motor and the zero order hold is given by

$$G(z) = \frac{(1 - e^{-aT})}{(z - e^{-aT})} \tag{6}$$

where

D viscosity coefficient of the shaft
J moment of inertia
T sampling interval
a D/J.

The speed controller employs proportional plus integral action

$$d(t) = K\left[e(t) + \frac{1}{T_I}\int e(t)\,dt\right]. \tag{7}$$

In the z domain, this PI control action is given by

$$D(z) = (K_p + K_I)\cdot\frac{z - K_p/(K_p + K_I)}{z - 1} \tag{8}$$

where K_p is the proportional gain, and K_I is the integral gain.

The open-loop transfer function of the system is therefore

$$D(z)G(z) + (K_p + K_I) \cdot \frac{(1 - e^{-aT})\left[z - K_p/(K_p + K_I)\right]}{(z - 1)(z - e^{-aT})}. \tag{9}$$

The desired response of the drive system is obtained by the pole placement method. In this method, the desired closed-loop poles are located on the z plane for the desired response from the drive, and by adjustment of the controller parameters (K_p and K_I), the root locus of the drive system can be made to pass through the desired closed-loop poles. The values obtained for K_p and K_I then serve as a guide for further tuning.

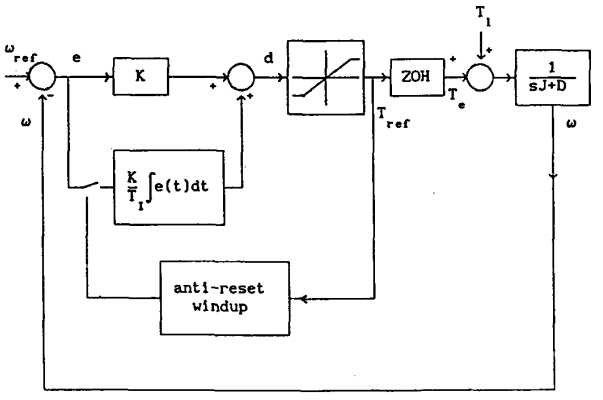

Fig. 3. PI speed controller.

C. Position Control

A position control algorithm is implemented as the outer loop controller to test its performance when integrated with the instantaneous torque controller. This control algorithm is based on variable structure strategy. It had been implemented in a BLDC drive system with conventional pwm current control and reported in an earlier publication [12]. To have a well-damped response with no overshoot, the following switching function is used:

$$s = cx_1 + x_z \tag{10}$$

where x_1 is the position error, and $x_z = x_1$.

The VSS control function implemented is

$$u = \psi_1 x_1 + \psi_2 x_2 + k_f \operatorname{sgn}(s) \tag{11}$$

where

$$\psi_1 = \begin{cases} \alpha_1, & \text{if } sx_1 > 0 \\ \beta_1, & \text{if } sx_1 < 0 \end{cases}$$

$$\psi_2 = \begin{cases} \alpha_2, & \text{if } sx_2 > 0 \\ \beta_2, & \text{if } sx_2 < 0 \end{cases}$$

$$\operatorname{sgn}(s) = \begin{cases} 1, & \text{if } s > 0 \\ -1, & \text{if } s < 0. \end{cases}$$

The first term in (11) is like a normal proportional term, the second term is a form of velocity feedback, and the third term is a relay type term that is commonly used in control systems to overcome the effects of backlash and coulomb frictional forces.

The VSS control system in the sliding mode must satisfy the existence condition

$$\lim_{s \to 0} s\dot{s} < 0. \tag{12}$$

A sufficient condition is that the gain constants satisfy the following inequalities:

$$\begin{cases} -(1/J)\alpha_1 < , & \text{if } sx_1 > 0 \Rightarrow \alpha_1 > 0 \\ -(1/J)\beta_1 > 0, & \text{if } sx_1 < 0 \Rightarrow \beta_1 < 0 \end{cases}$$

$$\begin{cases} c - (\alpha_2 + D)/J < 0, & \text{if } sx_2 > 0 \Rightarrow \alpha_2 > (cJ - D) \\ c - (\beta_2 + D)/J > 0, & \text{if } sx_2 < 0 \Rightarrow \beta_2 < (cJ - D) \end{cases}$$

$$-(k_f/J)|s| + s \cdot f(x,t) < 0$$

$$k_f > T_L \operatorname{sgn}(s).$$

Thus, $k_f > T_L$.

α_1 and β_1 are easily chosen to satisfy the above conditions and are significant when the error is large and negligible when the error is small. The value of α_2 is chosen with maximum inertia, whereas β_2 is chosen with minimum inertia. The value of k_f is selected with maximum load torque T_L.

III. Hardware Implementation

The digital control strategies proposed in Section II have been implemented with a digital signal processor: the DSP32 manufactured by AT&T [13]. This particular device is chosen because the torque control and torque estimation algorithms require very fast computations in order to limit chattering of the phase currents. The DSP32 is supported by a microcomputer that serves as a host development system during the development of the control application programs and provides input/output facilities during real-time testing of the programs. This allows for speedy program development, debugging, and testing. It is also versatile and can be expanded into a multimotor controller. For a practical commercial design, the DSP can be permanently masked programmed with the fully tested application programs and provided with its I/O facilities so that it can operate as a standalone controller.

IV. Controller Performance

A. Speed Control

Both the sinusoidal current control and the instantaneous torque control are tested with the speed controller. Four sets of tests have been conducted for each control scheme combination. The test conditions are shown in Table III. The sampling time for the speed controller is chosen to be 1 ms.

The time responses of the system for a step speed command are shown in Figs. 4 to 7. The results show that speed ripples are negligible for the combination of PI speed control and instantaneous torque control. Large variations in speed occur for the speed and sinusoidal current control combination, especially at very low speeds. The settling times and speed ripple factors (SRF's) for all the tests are tabulated in Table IV. Settling time is defined as the time taken for the response curve to reach within 5% of the final value. SRF's are defined as the ratio of peak-to-peak speed ripple to the mean speed:

$$\text{SRF} = \frac{\delta\omega_{pp}}{\omega_{\text{mean}}}. \tag{13}$$

The settling times for speed control with instantaneous torque control are more consistent in the presence of load variations, and the SRF's are always smaller. From the results, it can be

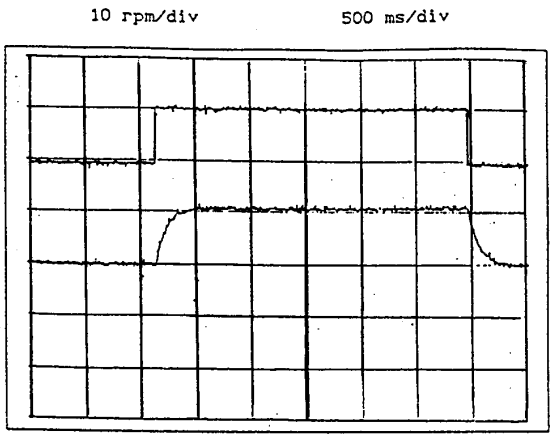

(a)

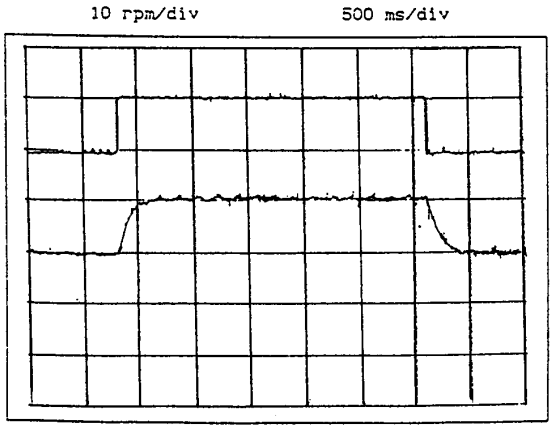

(b)

Fig. 4. Experimental results for speed control; test 1: (a) With instantaneous torque control; (b) with sinusoidal current control.

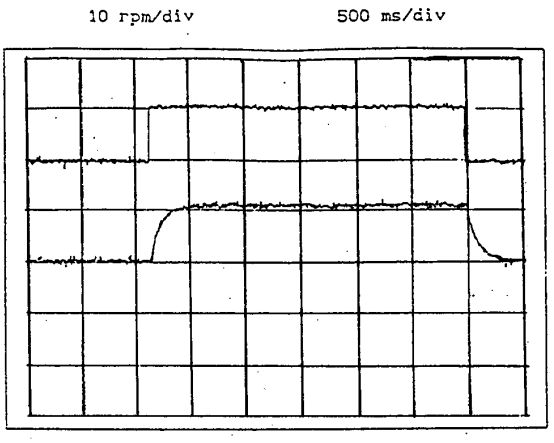

(a)

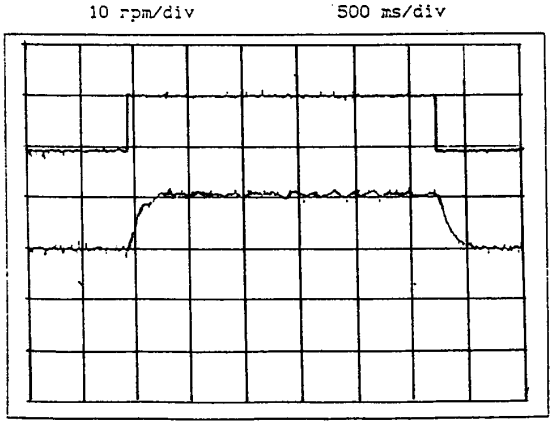

(b)

Fig. 5. Experimental results for speed control; test 2: (a) With instantaneous torque control; (b) with sinusoidal current control.

seen that instantaneous torque control has improved the transient and steady-state responses of BLDC drive for speed control applications.

B. Position Control

The performance for position control are also obtained using both sinusoidal current control and instantaneous torque control. The results are shown in Figs. 8 and 9 for two different loading conditions. In both cases, overshoots are observed for the position curves obtained using sinusoidal current control. The instantaneous torque control scheme exhibits fast but well-damped responses with no overshoot. The incorporation of instantaneous torque control in the inner loop has improved the transient performance of the position controller.

C. Static Torque Control

The instantaneous torque control scheme proposed can control the developed torque on the motor shaft even when the shaft is stationary. In this test, the shaft of the rotor is

TABLE III
TEST CONDITIONS FOR SPEED CONTROL $K_p = 1.20$, $K_I = 0.05$

Test No.	Test Conditions
1	speed reference = 10 r/min, load = 0.15 Nm
2	speed reference = 10 r/min, load = 0.55 Nm
3	speed reference = 1 r/min, load = 0.15 Nm
4	speed reference = 1 r/min, load = 0.55 Nm

TABLE IV
SPEED CONTROL PERFORMANCE INDICES

	Sinusoidal Current Control		Instantaneous Torque Control	
Test No.	Settling Time (sec)	SRF	Settling Time (sec)	SRF
1	0.35	0.09	0.32	0.03
2	0.25	0.15	0.32	0.06
3	0.21	0.25	0.23	0.10
4	0.17	0.26	0.23	0.11

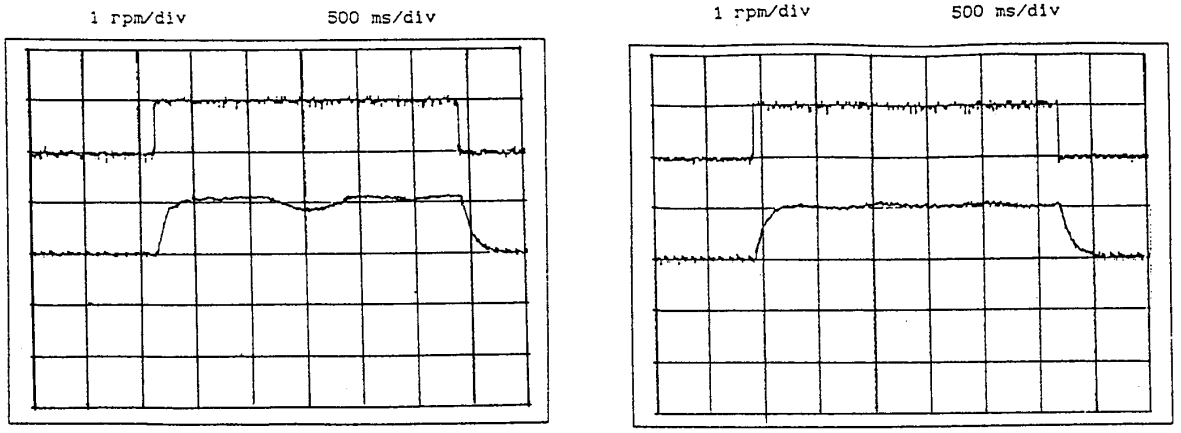

(a) (b)

Fig. 6. Experimental results for speed control; test 3: (a) With instantaneous torque control; (b) with sinusoidal current control.

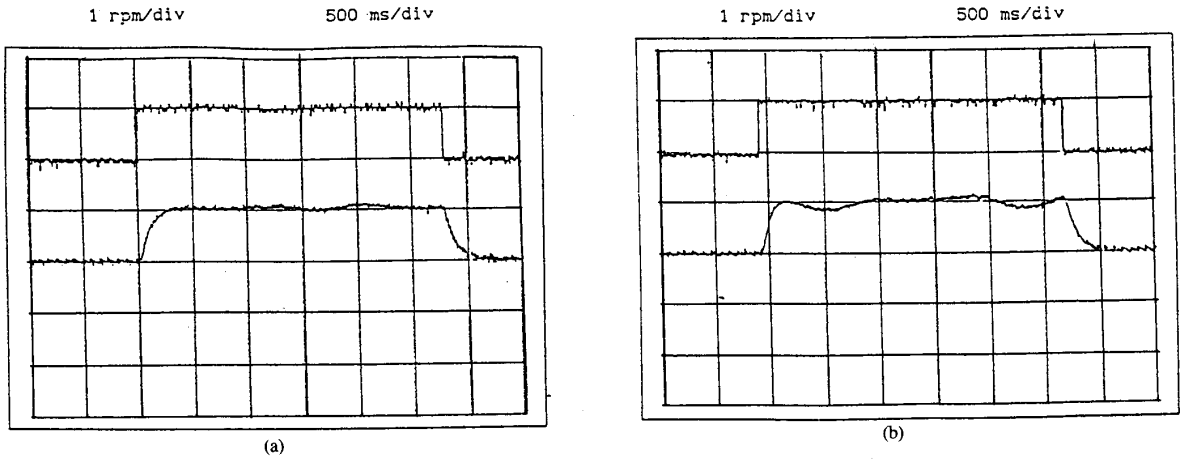

(a) (b)

Fig. 7. Experimental results for speed control; test 4: (a) With instantaneous torque control; (b) with sinusoidal current control.

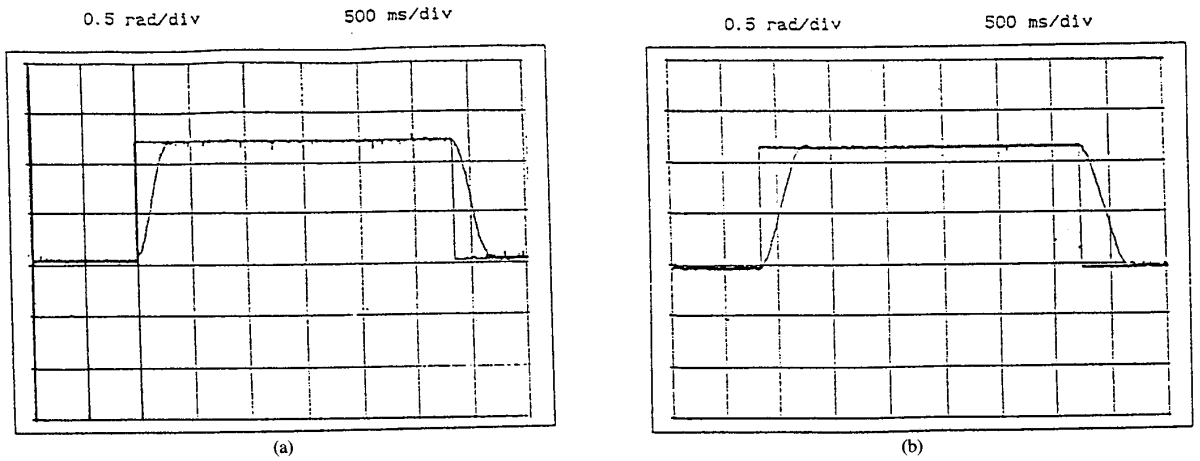

(a) (b)

Fig. 8. Experimental results for position control (no load): (a) With instantaneous torque control; (b) with sinusoidal current control.

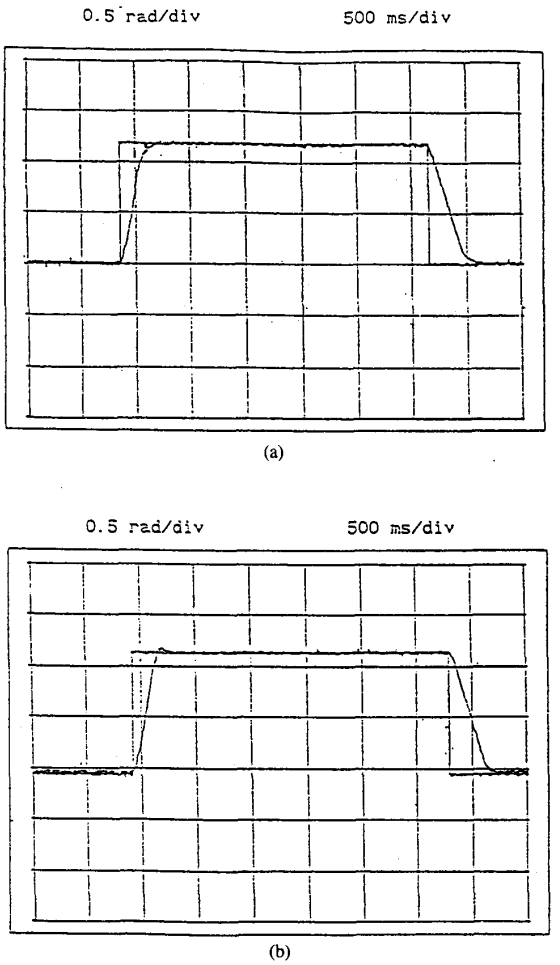

Fig. 9. Experimental results for position control (load = 2 Nm): (a) With instantaneous torque control; (b) with sinusoidal current control.

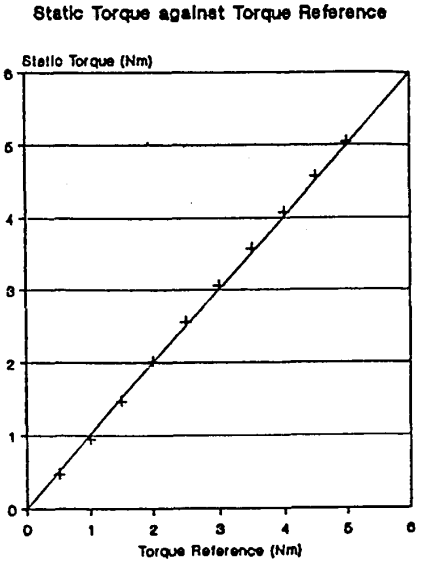

Fig. 10. Static torque versus torque reference.

TABLE V
STATIC TORQUE CONTROL (ALL FIGURES IN NM)

Torque Reference	Shaft Torque	Absolute Error
0.0	0.0	0.0
0.5	0.47	0.03
1.0	0.95	0.05
1.5	1.47	0.03
2.0	2.02	0.02
2.5	2.56	0.04
3.0	3.06	0.06
3.5	3.58	0.08
4.0	4.07	0.07
4.5	4.58	0.08
5.0	5.05	0.05

locked in a fixed position. The instantaneous torque control scheme is used to control the static torque for a range of torque references. The developed torque is measured by a torque transducer. The readings are tabulated in Table V. and plotted in Fig. 10. The results show that the accuracy of the developed static torque is accurate within the working range of the motor to 94%.

V. CONCLUSIONS

The concept of instantaneous torque control has been introduced for BLDC drive control as an alternative to the conventional sinusoidal current control with the aim of minimization of torque pulsations and optimal useful torque production. The torque control algorithm is based on variable structure strategy. This has been implemented on a DSP-based controller.

The performances of the BLDC drive for servo applications using instantaneous torque control have been examined. In all these applications (speed control, position control, and static torque/force control), the results show that the instantaneous torque control has improved the performances when compared with a system with sinusoidal current control. Static torque/force control has also been shown to be accurate.

REFERENCES

[1] T. S. Low, K. J. Binns, M. F. Rahman, and L. B. Wee, "A Nd-Fe-B excited permanent-magnet motor—Design and performance," in *Proc. 3rd Int. Conf. Elect. Machines Drives, IEE* (London), Nov. 16-18, 1987, pp. 246-249.

[2] T. S. Low, "Permanent-magnet motors for direct drive applications," *Automation News*, pp. 14-17, Nov. 1987.

[3] H. Asada, T. Kanade, and I. Takayama, "Control of a direct drive arm," *Trans. ASME*, vol. 105, pp. 136-142, Sept. 1983.

[4] S. Davies and D. Chen, "High performance brushless dc motors for direct drive robot arm," *PCIM*, pp. 35-38, Aug. 1985.

[5] L. Hoang, R. Perret, and R. Feuillet, "Minimization of torque ripples in brushless dc motor drives," *IEEE Trans. Industry Applications*, vol. IA-22, no. 4, pp. 748-755, July 1986.

[6] B. H. Ng, T. S. Low, K. W. Lim, and M. F. Rahman, "An investigation into the effects of machine parameters on the torque pulsations in a brushless dc drive," in *Proc. 1988 Cong. Ind. Elect.* IECON '88 (Singapore), Oct. 24-28, 1988, pp. 749-754.

[7] T. S. Low, T. H. Lee, K. J. Tseng, and K. S. Lock, "A strategy for the instantaneous torque control of permanent-magnet brushless dc drives," in *Proc. Inst. Elec. Eng., Pt. B*, vol. 137, no. 6, pp. 355-363, Nov. 1990.

[8] K. J. Tseng, T. S. Low, and K. S. Lock, "Torque control in permanent-magnet brushless dc drives," in *Proc. Symp. Motion Control* (Singapore), Apr. 6, 1989, pp. 12-30.

[9] T. S. Low, K. J. Tseng, K. S. Lock, and K. W. Lim, "Instantaneous torque control," in *Proc. 4th Int. Conf. Elect. Machines Drives* (London), Sept. 13-15, 1989, pp. 100-105.

[10] B. H. Ng, "An investigation into the effects of machine parameters on the torque pulsations in a brushless dc drive," M.Eng thesis, Nat. Univ. Singapore, 1988.

[11] M. F. Rahman, T. S. Low, and L. B. Wee, "Development of a digitally controlled brushless dc drive system," in *Proc. 1986 Conf. Appl. Motion Control* CAMC '86 (Minneapolis, MN), June 10-12, 1986, pp. 283-288.

[12] L. B. Wee, K. W. Lim, T. S. Low, and M. F. Rahman, "A variable structure strategy for motion control," in *Proc. 1987 Conf. Ind. Electron.* IECON '87 (Cambridge, MA), Nov. 3-6, 1987, pp. 167-174.

[13] *WE DSP32 Digital Signal Processor Information Manual*, AT&T Documentation Management Organization, Sept. 1986.

Teck-Seng Low received the B.Sc. degree with First Class Honors in electrical engineering from the University of Southampton, England, in 1978. He received the Ph.D. degree from the same university in 1982.

He was a research fellow at the University of Southampton before joining the National University of Singapore in 1983 as a lecturer. He is presently a senior lecturer, and his research interests include the design and control of permanent magnet motors, robotics, and the application of neural networks in machine design and control.

Tong-Heng Lee received the B.A. degree with First Class Honors in the engineering tripos from Cambridge University, England, in 1980 and the M.Sc. and Ph.D. degrees from Yale University, New Haven, CT, in 1984 and 1987, respectively.

From 1982 to 1983, he worked as a research engineer at the National University of Singapore, investigating methods of on-line parameter estimation. His Ph.D. work at Yale was in the area of adaptive systems theory. Currently, he is a Senior Lecturer at the Department of Electrical Engineering of the National University of Singapore. He teaches both undergraduate and graduate courses in control systems engineering. His research interests include applications of expert systems for control and issues in the design of controllers for fast servo systems.

Dr. Lee was awarded the Baker Prize by the Cambridge University Electrical Engineering Department in 1980.

King-Jet Tseng received the B. Eng. (First Class) and M. Eng. degrees from the National University of Singapore in 1988 and 1990, respectively.

His research was in motion control. He is currently at Cambridge University, Cambridge, England.

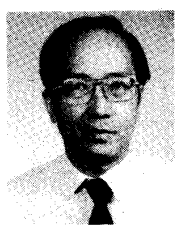

Kai-Sang Lock received the B.Sc and Ph.D degrees from the University of Strathclyde, UK.

He joined the National University of Singapore in 1980 and is currently a Senior Lecturer in the Department of Electrical Engineering. His areas of interest are power electronics, electric drives, motion control, and power system harmonics. He has taken a number of industrial consultancy projects related to these areas.